

# KSTAR ECH System Development Progress

Mi Joung<sup>1\*</sup>, Sonjong Wang<sup>1</sup>, Sunggug Kim<sup>1</sup>, Jongwon Han<sup>1</sup>, Inhyuk Rhee<sup>1</sup>, and Jonggu Kwak<sup>1</sup>

<sup>1</sup>Korea Institute of Fusion Energy (KFE), Daejeon, South Korea

**Abstract.** The KSTAR ECH system has been upgraded to ensure steady-state advanced operation of KSTAR. The planned ECHs include a total of six 1 MW, 300 s ECH systems, of which four 105/140 GHz dual frequency systems have been commissioned and are being used in KSTAR experiments. Additionally, a 170 GHz Russian gyrotron has been commissioned and is ready for injection. The final unit, a multi-frequency gyrotron similar to Japan's ITER gyrotron, is scheduled for installation and operation in early 2025. To achieve the KSTAR mission of high-performance long-pulse operation using a plasma operation scenario with a high poloidal beta, ECH requires stable and long pulses, which typically results in the reduction of ECH power during campaigns. Consequently, one ECH unit with power ranging from 0.5 to 0.7 MW was utilized in the KSTAR experiments. The ECH power and launching angle can be controlled by the Plasma Control System (PCS) which maximizes the ECH effect at startup and at the flat top of the discharge. This paper describes the development status of the KSTAR ECH system and reports the long-pulse operation results of the ECH system for a dummy load and KSTAR.

## 1 Introduction

The Korea Superconducting Tokamak Advanced Research (KSTAR) is a medium-sized superconducting tokamak. The main mission of KSTAR project is to explore the physics and technologies of high-performance steady-state operations in preparation for ITER and K-DEMO [1]. The targeted normalized beta  $\beta_N$  is over 3.0 and the H-mode pulse duration is 300 s. Fully non-inductive current-drive operation is required to achieve steady-state operation for 300 s. A three-stage research plan was established to support this mission. In the second phase of the KSTAR project, the final plan for the heating and current drive system was confirmed to be 12 MW for NBI and 6 MW for ECH. The NBI, which is the main heating and current drive source in KSTAR, was planned to 6 MW of on-axis tangential injection and 6 MW of off-axis tangential injection. The ECH has a plan to consist of four 105/140 GHz dual frequency systems and two 170 GHz systems. Each output has been gradually increasing. In the third phase, a tungsten diverter system was designed and manufactured according to the KSTAR research plan for steady-state and reactor-relevant research. After the 2022 campaign, the lower diverter was successfully converted into an actively cooled tungsten monoblock diverter with a designed peak heat flux of 10 MW/m<sup>2</sup> [2].

The ECH system, one of the main heating and current drive systems in KSTAR, plays crucial role in plasma startup and flux saving in superconducting devices with low loop voltage [3, 4]. KSTAR has routinely used ECH-assisted startups, and although these startups have occasionally failed, ECH was utilized for wall conditioning by the ECWC [4, 5]. Furthermore, long-

pulse operation, a key mission of KSTAR, significantly benefits from ECH. This operation has been achieved using a high  $\beta_p$  discharge scenario, which helps to increase the non-inductive current fraction [6]. In this scenario, ECH injection has improved the non-inductive current fraction by precisely controlling the deposition location and toroidal angle of ECH in KSTAR. Pulse lengths have gradually increased since 2015, when a pulse length of 60 s was achieved. In the last campaign, with the new lower tungsten diverter installed, KSTAR achieved a new record of 102 s by operating two 105 GHz ECH systems into the H-mode plasma based on NBI power. To date, four 105/140 GHz dual frequency gyrotrons and one 170 GHz gyrotron have been installed and commissioned at KSTAR. This paper explains the development status of the KSTAR ECH system for long-pulse operation in Section 2, while Section 3 presents long-pulse operation results of the 105/140 GHz ECH system in the dummy load and 102 s operation results in KSTAR.

## 2 Status of KSTAR ECH system

Six ECH systems—four 105/140 GHz dual frequency systems and two 170 GHz systems—were planned for high-performance, steady-state operation in KSTAR. Each system was designed to operate independently, complete with its own auxiliary system, power supply, transmission line, dummy load, and launcher. Details of the KSTAR ECH system design are discussed in reference [7], while this paper focuses on the development status of the components for long-pulse and high-power operation. The KSTAR ECH system was upgraded for high-performance steady-state

\* Corresponding author: [whitemi@kfe.re.kr](mailto:whitemi@kfe.re.kr)

operation, with each system capable of handling 1 MW of power for 300 s and operating stably at KSTAR. As high-power microwave sources, gyrotrons face major limitations in terms of injection power and pulse duration. The power output from the gyrotron window can lose up to 10 % at the MOU. This value can be reduced by the high mode purity of the output beam in the gyrotron window. The EC wave generated by the gyrotron is transferred to the launcher or switched to a dummy load to measure the power or to condition the gyrotron. The dummy load was placed immediately before the entrance to the tokamak hall. The transmission line (TL) was designed to minimize the number of miter bends to reduce transmission loss. Seven miter bends, two power monitors, one pair of polarizers, and two arc detectors were used in each system. It can handle a 1 MW CW operation that is directly cooled by water, except for waveguide, which is cooled by water jackets. Finally, the theoretical losses were 6.6/5.7/4.9% for each frequency, 105/140/170 GHz, respectively.

To date, four 105/140 GHz dual frequency gyrotrons and one 170 GHz gyrotron have been installed and commissioned at KSTAR. Of these, four 105/140 GHz gyrotrons have been operated in KSTAR experiments, but the 170 GHz gyrotron has not yet been operated due to unusual heat load in the cavity and MOU. Moreover, three of the four 105/140 GHz gyrotrons were repaired due to RF power degradation, water leakage at the window, and gyrotron heater malfunction caused by errors in the automation procedures. Up to three ECH systems have been operated simultaneously, producing an output power of approximately 1.5 MW. We are working diligently to ensure stable and reliable operation of the gyrotron system.

The last gyrotron, a multi-frequency gyrotron procured from Kyoto Fusioneering, Japan, similar to the ITER gyrotron, can operate at three frequencies—170, 137, and 104 GHz—without breaking the vacuum of the TL. This will be beneficial for KSTAR startups. It is scheduled to be delivered and become operational in 2025.

The ECH control system was also upgraded to ensure the safe and reliable operation of the ECH system [8]. Figure 1 shows the configuration of the main KSTAR ECH control system, used to determine the control logic. This system, called the ECFC, receives four inputs for arbitrary power modulation (fM, dM, HM, LM, corresponding to modulation frequency, duty cycle, high output, and low output, respectively) and an LTU signal to control the high-voltage power supplies CPS and BPS. The ECFC, based on D-Tacq's field-programmable gate array (FPGA) with sampling rates of up to 2 MHz for real-time control and RF modulation of up to 5 kHz, includes a re-trigger function and a feature that adjusts the EC power during the plasma discharge. The EC power can also be modulated into arbitrary waveforms, a capability used to study the EC power threshold and real-time plasma control. Figure 1(b) shows an example of RF power control using the ECH controller.

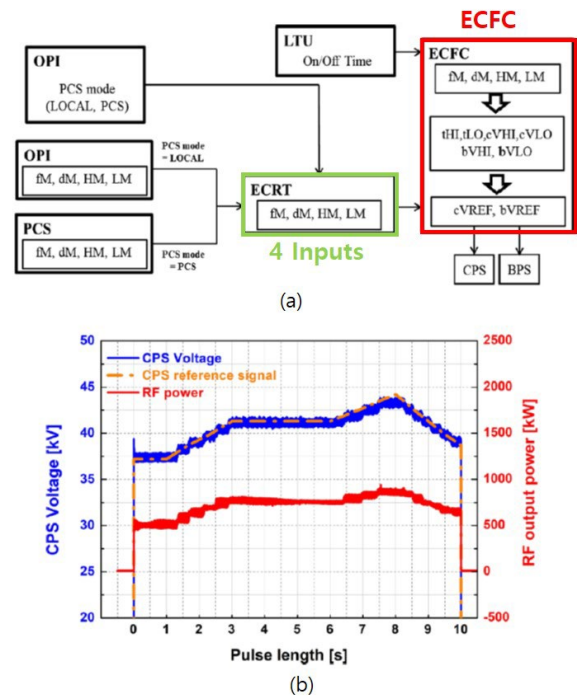


**Fig. 1.** (a) Block diagram of new ECH main control system and (b) an example of RF power control by new ECH control system

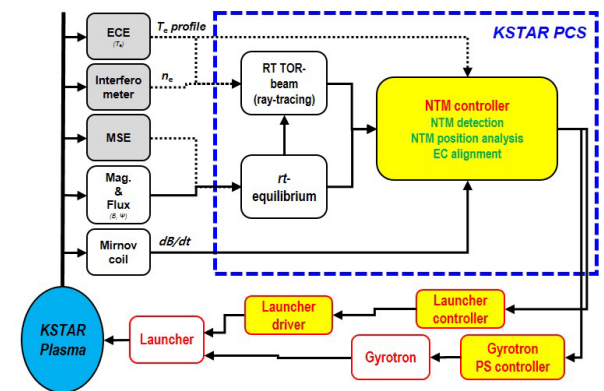


**Fig. 2.** NTM control system with ECH power and launcher control in KSTAR PCS. Dotted lines indicate that they are not yet connected.

The ECH launchers consist of two 1-beam launchers and two 2-beam launchers. The two 1-beam launchers were designed and fabricated in collaboration with PPPL [9]. The configuration and operating mechanism of two-beam launcher was essentially identical with 1-beam launcher, but the size and scanning angle of a front-steerable mirror were slightly increased. The ECH launcher and power control logic were integrated into the KSTAR Plasma Control System (PCS) system for NTM control, as shown in Figure 2, and could be operated independently. For the launcher, the poloidal position or the toroidal angle can vary respectively depending on the experiment's objectives. A typical ECH-assisted startup involves on-axis heating, and on a flap top, it is possible to vary the entry position or toroidal angles. Although on-axis heating is essential on a plasma flat top, the launcher angles can be optimized for the plasma current and shape. This

launcher control system had a scan speed of 50 cm/s and a latency of 10 ms. The launcher controller was slightly modified to ensure safe operation. The system was divided into a controller and a driver, with the controller located outside the tokamak room to prevent malfunctions during the KSTAR experiments.

The other modification to the launcher was the cooling mechanism of the steering mirror. We recently adopted copper thermal straps, passive heat transfer devices consisting of two end fittings and a bunch of flexible heat links connecting them, to cool the steering mirror and extend its lifecycle. Figure 3 shows the new steering mirror assembly with copper thermal straps and simulation results of temperature distribution and temperature changes over time of this assembly. Under conditions where 1 kW of power was absorbed by the mirror for 100 s, the temperature rise of the steering mirror was approximately 180 K, and it took approximately 1 hour to return to the initial temperature. This mechanism can reduce coolant leaks; however, potential thermal deformations have not yet been fully considered. Thermal deformation must be monitored during long-pulse operations.

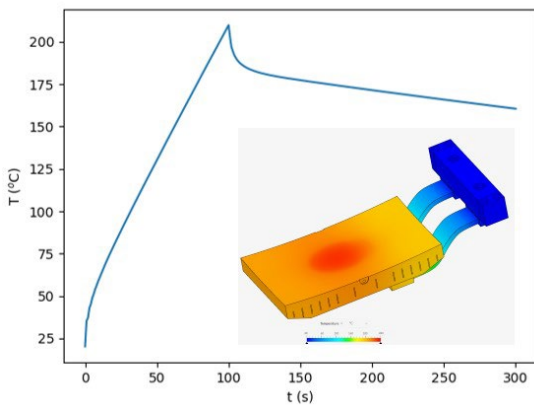


**Fig. 3.** Newly designed steering mirror assembly with copper thermal straps for indirect cooling and simulation results of temperature distribution and changes of this assembly by absorbing 1 kW of power for 100 s.

### 3 Experimental results of KSTAR ECH system

#### 3.1 300 s operation to the dummy load

Before the 300 s operation of the gyrotron, it is essential to verify the alignments of the gyrotron with the magnetic field and the output beam with the TL. Aligning the output beam with the TL is challenging in certain cases, primarily due to poor mode purity, which complicates the definition of the beam's centre. Furthermore, longer pulse operations may not be achievable due to abnormal temperature increases in some components, resulting in reduced efficiency and unforeseen disruptions. Once this alignment is ensured, the pulse length was initially increased to 300 s at low power, followed by a stepwise increase in power. For the 140 GHz operation, we utilized a heater boost to maintain a higher beam current and RF oscillation. However, a heater boost was not required for 105 GHz

operation. During the increase in pulse length or power, the calorimetric power at critical points and the temperature rise of the TL were monitored. Figure 4 illustrates the temperature rise of the TL components during the 300 s operation at 105 GHz EC4 operation, achieving approximately 700 kW at the dummy load. The measured positions include the first power monitor miter bend (PM1), first polarizer miter bend (Pol1), the waveguide between PM1 and Pol1 (mid), the waveguide switch input port and diverted port (WG SW in and div.), along with the second and third plain miter bends (MB2 and MB3) from the MOU to the dummy load, marked with the same coloured letters. Higher losses were observed at the waveguide switch. However, the theoretical loss of waveguide switch is similar to that of a plain miter bend but lower than that of a polarizer miter bend. These results are very similar to those at the 140 GHz frequency. The discrepancies may be due to TL misalignment, beam misalignment, or the higher-order mode of the beam; therefore, further analysis is necessary. We typically adjust the location of the water jacket to keep the waveguide temperature below 100 °C. However, in this instance, the switch temperature exceeded 110 °C at 105 GHz. For longer-pulse operations, such as those planned for ITER, which aims to operate for 1000 s in the future, improvements in the cooling method of the waveguide are required.

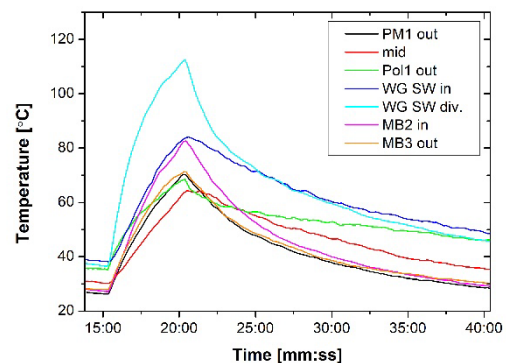


**Fig. 4.** Temperature in the TL to the dummy load during 300 s operation (105 GHz, 700 kW, EC4)

#### 3.2 100 s operation to KSTAR

As mentioned in Section 2, the ECH must be prepared for long-pulse operation at KSTAR. ECH plays a crucial role in extending the pulse duration of the H-mode plasma in KSTAR. Therefore, to ensure stable long-pulse operation, the output power of the gyrotron is often reduced not only during the commissioning of the gyrotron system before the KSTAR experiments but also during the experimental campaigns. Figure 5 displays the results of a high-performance long-pulse operation lasting 102 s, the longest newly recorded shot, achieved with the newly installed W-lower diverter in the last campaign. This new record was attained by applying a real-time MD linear drift correction algorithm to the PCS and optimizing the plasma shape as shown in Figure 6(a). Figure 5 shows typical waveforms of plasma parameters with a plasma current ( $I_p$ ) of 400 kA, external NBI and ECH power ( $P_{NBI}$  and

$P_{EC}$  of 4 MW and 1 MW respectively, poloidal beta ( $\beta_p$ ) of 2.5, normalized beta ( $\beta_N$ ) of 2.0, loop voltage ( $V_{loop}$ ) of approximately 0.07, line averaged electron density ( $n_{e,core}$ ) of  $3 \times 10^{19} \text{ m}^{-3}$ , and  $D_\alpha$ . The loop voltage was very low but not zero, indicating not a fully non-inductive discharge. A fully non-inductive current drive is required to further extend the pulse length. In these experiments, 2<sup>nd</sup> harmonic X-mode ECHs (EC4 and EC5) were injected at a major radius of  $R_{res}=1.87 \text{ m}$ , and a vertical position of  $z=0$  as shown in Figure 6(b). The EC5 power was controlled by the PCS for ECH-assisted startup. Each ECH had a power of approximately 600 kW, with a total of 1.2 MW injected. It remained very stable without any faults. ECH proved essential for these experiments because when ECH was turned off, the loop voltage increased, both  $\beta_p$  and  $\beta_N$  decreased, and  $D_\alpha$  increased, as shown in Figure 7. Therefore, when ECH is turned off, the plasma is typically stopped manually.

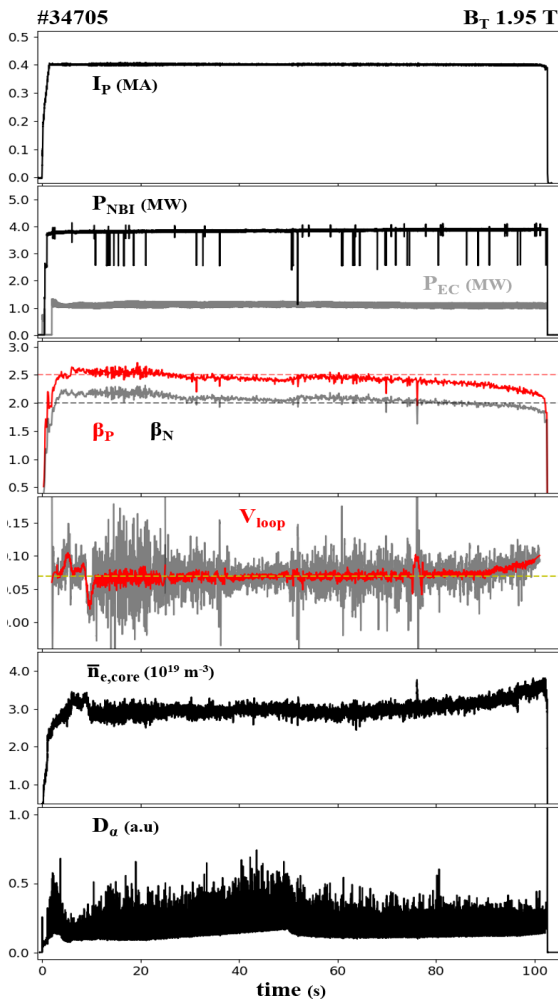


**Fig. 5.** Waveforms of plasma parameters for the 102 s high-performance long-pulse operation

In shot #34705, we evaluated the performance and behavior of the TL components used only when injecting the EC beam into KSTAR. These components included two arc detector miter bends (Arc MBs), a waveguide between the two Arc MBs (mid), a pump-out tee (pump-out), a second power monitor miter bend

(PM2), an RF gate valve (RF GV), bellows, a DC break, and a launcher waveguide adaptor input (Launcher in). Figure 8 shows the temperature traces at the input or output of each component during the #34705 discharge. As mentioned in Section 3.1, the temperature at the output of the waveguide switch was higher than at the output of Arc MB2. Unusually, the temperature at Arc MB2 increased by almost two orders of magnitude compared with the other miter bends. We believe this was due to misalignment. After the campaign, we observed minor vacuum leakage near this point. The temperatures of the other components near the launcher, including the RF GV, DC break, and bellows, did not increase significantly.

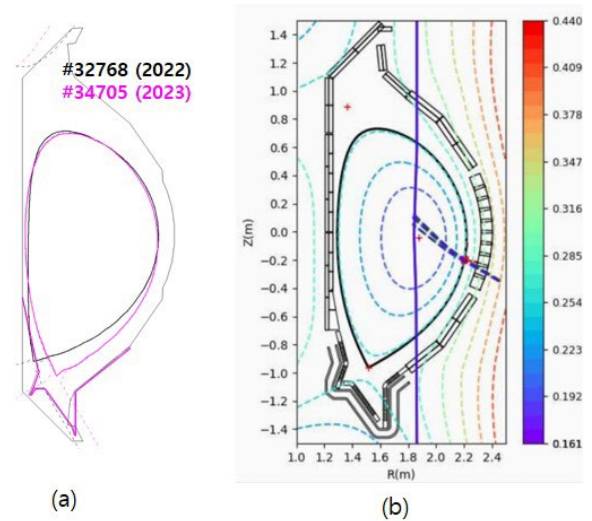


**Fig. 6.** (a) Comparison of the last closed flux surfaces of discharge #32768 and discharge #34705 with the newly installed W-lower diverter (bold pink line) and (b) equilibrium and Toray ray tracing result of EC4 and EC5.

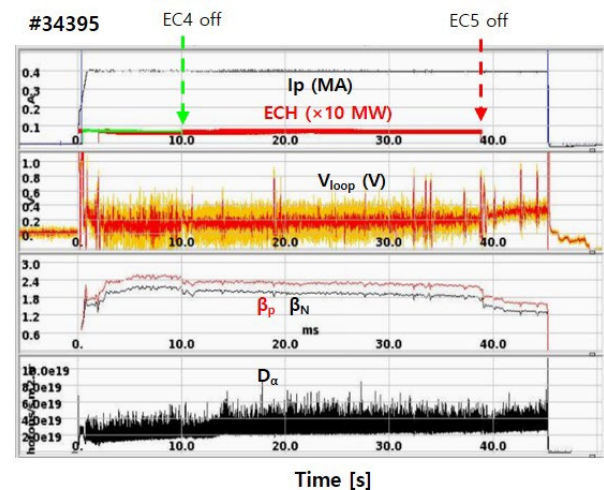


**Fig. 7.** Waveforms of plasma parameters for the long-pulse plasma where ECH was turned off by some events during the pulse.

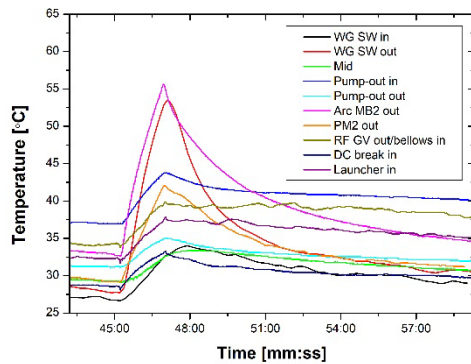


**Fig. 8.** Temperature traces of TC sensors installed from the RF waveguide switch to the launcher when ECH power (105 GHz, EC4) was injected into KSTAR (#34705).

## 4 Conclusion

The KSTAR ECH system has been improved to ensure high-performance and steady-state operation of KSTAR. To date, four 105/140 GHz ECH systems have been operated, and one 170 GHz system has been commissioned and is ready for operation at KSTAR. The ECH system was designed to operate for 300 s and has been confirmed to operate for 300 s using a dummy load. The re-trigger function was used to ensure continuous injection of ECH into KSTAR, and the angle or deposition position of the ECH beam could be adjusted during the pulse, allowing optimization according to the experimental purpose. KSTAR successfully performed a 102 s high-performance long-pulse operation in a tungsten divertor, where ECH with 1.2 MW power enabled flux saving and high-beta operation through on-axis heating at startup and flat top. The abnormal transmission loss observed during long-pulse operations will be resolved by improved alignment and mode purity. The final 170 GHz gyrotron will be installed and commissioned in 2025.

## References

1. G. S. Lee, et al., The design of the KSTAR tokamak, *Fusion Eng. Des.*, **46**, 405-411 (1999) [https://doi.org/10.1016/S0920-3796\(99\)00032-0](https://doi.org/10.1016/S0920-3796(99)00032-0)
2. W. C. Kim, S. H. Park, S. W. Kwag, et al., Key features of KSTAR's new tungsten divertor, ISFNT-15 (2023) <https://isfnt2023.com/wp-content/uploads/2023/12/PL6.pdf>
3. Y. S. Bae, J. H. Jeong, S. I. Park, M. Joung, et al., ECH pre-ionization and assisted startup in the fully superconducting KSTAR tokamak using second harmonic, *Nucl. Fusion*, **49**, 022001 (2009) 10.1088/0029-5515/49/2/022001
4. J. W. Lee, J. Kim, Y. H. An, et al., Study on ECH-assisted start-up using trapped particle configuration in KSTAR and application to ITER, *Nucl. Fusion*, **57**, 126033 (2017) 10.1088/1741-4326/aa8511
5. K. Itami, S. H. Hong, Y. S. Bae, M. Matsukawa, W. C. Kim, Wall-conditioning plasmas by ECRF

heating in KSTAR, *J. Nucl. Mater.*, **438**, S930-S935 (2013) 10.1016/j.jnucmat.2013.01.202

6. H. S. Kim, Y. M. Jeon, H. S. Han, et al., Development of high-performance long-pulse discharge in KSTAR, *Nucl. Fusion*, **64**, 016033 (2023) 10.1088/1741-4326/ad0fbd
7. M. Joung, S. J. Wang, et al., Design and operation results of KSTAR ECH system, *Fusion Eng. Des.*, **203**, 114461 (2024) <https://doi.org/10.1016/j.fusengdes.2024.114461>
8. Sunggug Kim, Sonjong Wang, Mi Joung, Jongwon Han, Inhyok Rhee, Development and status of high-voltage power supply and integrated control system for KSTAR ECH system, *Fusion Eng. Des.*, **175**, 112995 (2022)
9. Mi Joung, Minhoo Woo, Jongwon Han, et al., Design of ECH launcher for KSTAR advanced Tokamak operation, *Fusion Eng. Des.*, **151**, 111395 (2020)